Challenging Glass 5 – Conference on Architectural and Structural Applications of Glass
Belis, Bos & Louter (Eds.), Ghent University, June 2016.

ISBN 978-90-825-2680-6

Experimental and Numerical Investigation of Float Glass–GFRP Hybrid Beams

Bogdan Balan & Mithila Achintha
University of Southampton, United Kingdom, Mithila.Achintha@soton.ac.uk

Despite the great potentials of glass as a construction material, its brittle material behaviour poses major challenges to structural engineers when designing load-bearing glass structural members. This paper presents the load response and the failure behaviour of float glass–GFRP hybrid beams, when used as a mean of improving strength and ductility of float glass. Hybrid beams made from two layers of float glass sheets and an adhesively-bonded semi-transparent pre-cured GFRP interlayer were tested in four-point bending. The experimental results showed that double layer hybrid beams continued to take load even after the formation of the first major crack, and the beams were stronger and ductile than conventional single and multilayer float glass beams. Once the bottom glass layer has cracked the combination of the GFRP and the top glass layer carried the applied load whilst the gradual decrease in the stiffness due to the formation of new cracks ensures a ductile failure. Experimentally-validated finite element (FE) models that predict the evolution of stresses, stiffness and failure load of single and double layer glass beams, and glass– GFRP hybrid beams are also presented.

Keywords: Ductility, Finite Element Analysis, Float glass, GFRP, Glass Hybrid Beams, Stiffness

1. Introduction

Glass has traditionally been used as windowpanes in buildings, but owing to the innovative, energy efficient building envelops that glass can offer, the use of glass as a main building material became increasingly popular in the last 25 years (IStructE 2014). Glass is the most striking feature in modern building envelops. Despite the great potentials of glass as a construction material, its brittle material behaviour poses major challenges to structural engineers when designing load-bearing structural members, such as large areas of glass panels, roofs, floors, staircases and partitions. The structural behaviour of glass is significantly different to that of more familiar construction materials such as steel or reinforced concrete. In order to avoid brittle failures, the current industrial designs mostly over-design the glass structural elements.

One innovative way to eliminate brittle failure of glass is the use of glass–hybrid systems where a second material, such as steel (Nielsen and Olsen 2010, Louter et al. 2012), timber (Blyberg and Serrano 2011), or Fibre Reinforced Polymers (FRP) (Louter 2010, Speranzi and Agnetti 2015) is used as an external/internal reinforcement. The use of an adhesively-bonded or mechanically-connected additional material, which is stiffer and stronger (in tension) than glass, contributes to carrying tension in the hybrid beams. Although, glass–timber hybrids have been investigated (e.g. Blyberg and Serrano 2011), due to the poor durability and the complex interaction between the timber–adhesive bonds mean the use of timber is not as popular as the use of steel or FRP. In the beams studied in the literature, the reinforcing material was adhesively bonded and the direction of the loading was parallel to the glass layers of the beams (Fig. 1a). Nielsen and Olsen (2010) showed enhanced strength and ductility of float glass beams reinforced with an adhesively bonded steel strip at the bottom of the glass sheets. The beams showed an increased load capacity up to 25% compared to an unreinforced beam, and a ductile behaviour after the development of the first major crack. The experiments of Louter et al. (2012) on laminated glass beams reinforced with solid, steel sections at the tension surface showed that the post-fracture behaviour of the hybrid beams depend on the glass type and the amount of steel reinforcement.

Glass Fibre Reinforced Polymer (GFRP) has great potential as a reinforcing material in glass–hybrid beams due to high strength, lightweight and semi-transparent characteristics. The study of Louter (2010) showed GFRP rods embedded in between laminated glass beams enhanced the failure load of the beams tested in four-point bending. The hybrid beams showed a significant residual strength and ductile behaviour after the first crack. Recent studies (e.g. Correia et al 2011; Speranzi and Agnetti 2015) demonstrated the potentials of GFRP pultruded profiles to enhance the ductility of hybrid beams. The four-point bending tests done on the composites beams showed that by using float glass layers as web of an I-beam and the pultruded GFRP profiles as its flanges, an increase in strength of over five times of unreinforced beams can be achieved.

This paper reports experimental and numerical investigation of float glass–GFRP hybrid beams, in which a layer of GFRP bonded between two horizontal glass sheets (Fig. 1b). To the best of the authors' knowledge, at the time of writing (November 2015), the current work is the first study that investigates glass–GFRP hybrid beams with layers oriented perpendicular to the direction of the applied loads. The paper shows that the hybrid beams possess a greater ductility with a notable load carrying capacity even after the first cracking in the beam. The results show that the hybrid beams behaved elastically until the failure of the bottom glass layer, and once cracked, the GFRP layer carried the tensile force thereby enabling load carrying of the hybrid beam. Broken glass pieces remained stuck and interlocked on the GFRP layer, and this provided a significant post-fracture strength and prevented total failure of the hybrid beams compared to beams investigated in the literature where despite the increased strength and improved ductility the level of damage increases after the first major crack. The beams tested in the current study showed a significant recovery of the damage upon unloading.

The paper also numerically investigates the degree to which the strength and stiffness of hybrid beams can be modelled by using finite element (FE) models. The FE models were validated by comparing the predicted stresses in the glass beams with the experimental data obtain from strain gauges and the stresses measured using a scattered-light-polariscope (SCALP).

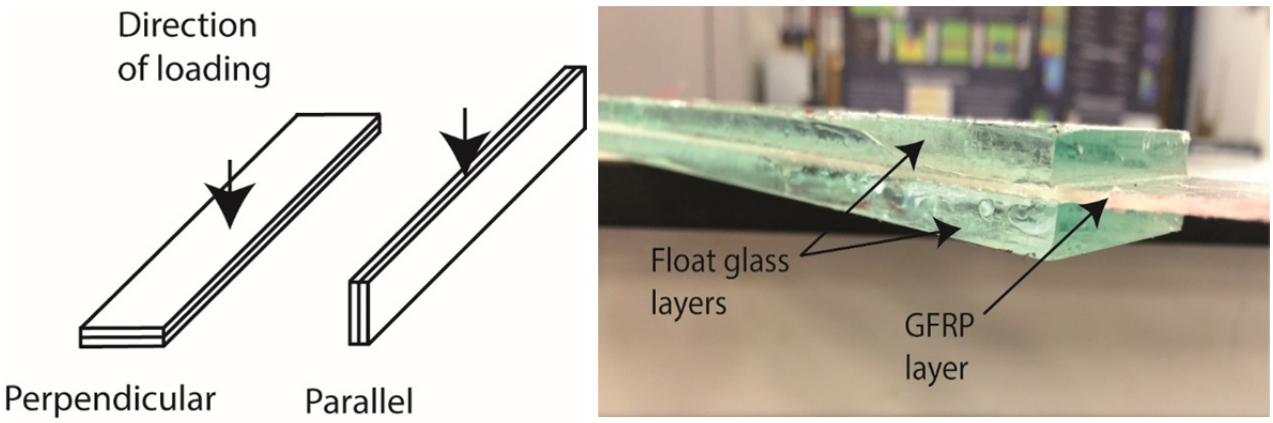

a) b)

Fig. 1 a) Orientation of the glass–GFRP hybrid beams, b) Layout of float glass–GFRP hybrid beams.

2. Materials and Test Specimens

The load response and the failure behaviour of glass–GFRP hybrid beams were investigated against single layer float glass beams and beams made of adhesively-bonded two layers of float glass sheets. Commercially available 6 mm thick float glass was used to fabricate the test beams of 600 mm long and 40 mm wide. The beams were tested in four-point bending with a constant moment zone of 400 mm long and two equal shear spans of 50 mm as shown in Fig. 2.

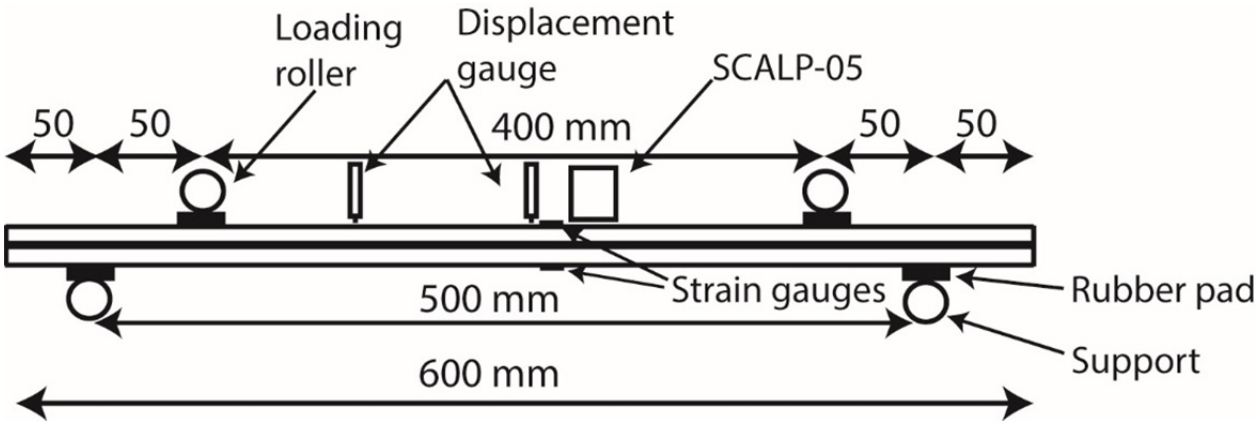

Fig. 2 Test setup configuration (All dimensions are in millimetres).

2.1 Single Layer Glass Beams

The glass beams were cut into size by a commercial service provider. An investigation using an optical microscope (Olympus CX22) showed that the edges were free from large defects whilst the microflaws, which were less than 600 μm long, were evenly distributed along the edges. A preliminary experimental investigation showed that the microflaws did not cause premature failure of the glass beams.

2.2. Double Layer Glass Beams

The double layer beams were made from two layers of 6 mm thick float glass bonded using clear structural adhesive, Araldite 2020. Araldite 2020 has the same refractive index as glass and has been widely used in industrial applications of joining glass members (Belis et al 2011). The mixing ratio used in the experiments was 100:50 by weight epoxy resin to hardener. Before the bonding of the second glass layer, each sheet was thoroughly cleaned and degreased with acetone. The total volume for required to obtain a 0.1 mm thick adhesive layer was evenly spread over the glass surface that was to be bonded. After joining the two glass sheets the beam was held together using a duct tape. The beams were then cured for 24 hours in an autoclave at 40 ± 1℃ and at the atmospheric pressure (~100 kPa). The beams were taken out of the autoclave after 24 hours and left to cure for another 6 days in laboratory conditions of 22 ± 3 ºC and atmospheric pressure. The thickness of each double layer beam was ~12. 1 mm.

2.3. Glass–GFRP Hybrid Beams

The Glass–GFRP hybrid beams (Fig. 1b) were made from two layers of 6 mm thick float glass and an adhesively bonded, semi-transparent pre-cured GFRP midlayer. The GFRP sheet had the same width as the glass layers (40 mm) but was 650 mm long compared to that of the glass sheets (600 mm). The GFRP strips were fabricated from a unidirectional GFRP E-glass dry fibre sheets (0.43 mm thick; 572 g/m^2). A wet lay-up system similar to the methods usually employed in practical civil engineering applications was used to fabricate the GFRP strips. A commercially available two-part epoxy resin, EL2 Epoxy Laminate Resin with AT30 slow hardener, was used. The fabricated GFRP strips were cured at room temperature (22 ± 3 ºC) and atmospheric pressure for 7 days. The average thickness of the final cured GFRP strip was ~1.35 mm and the fibre volume fraction was calculated to be ~50%.

Each glass sheet and the GFRP layer was thoroughly cleaned and degreased with acetone before bonding. The average thickness of the Araldite 2020 layer used on each side of GFRP was ~0.1 mm. After the fabrication of a hybrid beam a small pressure was applied to ensure a uniform distribution whilst the beams were tightened using a duct tape. The beams were then cured for 24 hours in an autoclave at temperature 40 ± 1℃ and at the atmospheric pressure (~100 kPa), after which they were left to cure for another 6 days in laboratory conditions of 22 ± 3 ºC and atmospheric pressure. The thickness of each double layer glass–GFRP hybrid beam was ~13. 5 mm.

2.4. Beam Test Setup

Three beam specimens of each beam type were tested in displacement controlled four-point bending 7 days after the fabrication of respective test specimen (Fig. 2). A servo-hydraulic test machine was used and quasi-static load at rate 1 mm/min was applied. 6 mm thick rubber pads were used under the loading rollers and at the supports to eliminate potential localised failures. A linear strain gauge each at the top (compression side) and the bottom (tension side) surface of each glass beam at the beam mid-span was used to measure strain data (Fig. 2). A scattered-light-polariscope (SCALP-05) (Achintha and Balan 2015) was also used to measure stress depth profiles in the constant moment zone of the beam specimens. The downward displacements at the beam midspan and at one-fourth location of the constant moment zone were continuously measured using digital displacement gauges (Fig. 2). The results of the experiments are presented in Section 5.

3. Finite Element Modelling

In order to develop a validated predictive tool to model the load response of the test beams, 3D FE models were developed using ABAQUS/Standard. The validation of the predicted load–displacement relationships and the predicted stress evolutions against the experimental data are presented in Section 5. It should be noted that it is common in the literature of FE analyses of structural adhesives to use complex models, which incorporate cohesive behaviour of the material as well as material/geometric nonlinearities. Whilst these appear to give a more appropriate representation of the adhesive–adherend interfaces, in practice the material parameters required are very difficult to determine. Since the current paper focuses on modelling the load-response of the hybrid beams before the failure it is appropriate to start with a simple model to represent the interfaces. Hence, in the current study, the materials were modelled as elastic solids, and full strain compatibility was assumed at the interfaces.

Fully integrated 3D solid elements (C3D8) were used to model all the materials. The analyses accounted for the large deformations of the beams. Appropriate element sizes required in the FE models were determined from a detailed mesh sensitivity analysis. Elements of dimensions of ~1 mm were used to model glass, whereas element sizes of ~0.35 mm and ~0.025 mm were used to model GFRP and adhesive respectively. It should also be noted that in order to minimise the artefacts of local stress concentrations in the vicinity of loading/support rollers, the applied

load and the support reactions were assumed to be distributed over 1 mm wide areas. A significant advantage of the FE models developed in this study is the incorporation of the effect of residual stresses in glass, which have often been ignored in the studies reported in the literature. The initial residual stress present in float glass was modelled using the eigenstrain based method previously developed by the present authors (Balan and Achintha 2015; Achintha and Balan 2015). The inclusion of the residual stress in the FE models will enable a better understanding of the load response of the beams.

4. Determination of the Mechanical Properties of the Materials

Glass and adhesive were assumed to be isotropic whereas GFRP was modelled as an orthotropic material with nonzero stiffness in the longitudinal direction only. The mechanical properties required in the FE models were the Young's modulus and Poisson's ratio of glass, GFRP (along the longitudinal direction) and Araldite 2020.

4.1. Glass

The Young's modulus and Poisson's ratio of float glass were assumed to be 70 GPa and 0.23 respectively in accordance with the widely reported literature (e.g. Haldiman et al 2008). Flexural tensile strength of glass was determined using the four-point bend tests and the results are discussed in the next section.

4.2. GFRP

The Young's modulus and the Poisson's ratio of the GFRP strips were determined from tensile tests carried out in accordance with ASTM D3039-95a (1995). Three GFRP specimens of 250 mm x 20 mm were tested in an electro-servo test machine at displacement rate of 2 mm/min. Linear strain gauges were used to measure strains in the longitudinal and transverse directions at the central region of the test specimens. As expected, a linear elastic behaviour was observed until the brittle failure. The stress–strain relationships of the three specimens are similar (less than 5% variance), and the average ultimate tensile strength, Young's modulus and the Poisson ratio were determined to be 450 MPa, 24.5 GPa and 0.10 respectively.

4.3. Araldite 2020

The tensile strength and the Young's modulus of the Araldite 2020 were determined in accordance with ASTM D638-02 (2002). Three identical tensile specimens of length 63 mm and thickness 3 mm were tested. A central gauge of length 7.62 mm and width 3 mm with a radius of fillet of 12.7 mm was used. The samples were first cured in an autoclave at temperature 40 ± 1 ºC and pressure 100 kPa for 24 hours, and were then cured in laboratory conditions (22 ± 3 ºC and atmospheric pressure) for further 6 days. The specimens were tested in direct tension at rate 1 mm/min 7 days after the fabrication. As can be seen from Fig 3a, the adhesive showed a largely linear behaviour until the ultimate tensile strength. A gradual drop in the load can be observed after the peak load. The ultimate tensile strength of the three specimens were determined to be 83.3, 91.1 and 93.3 MPa, giving an average value of 89.2 MPa. The Young's modulus of Araldite 2020 which is required in the FE analyses may be determined from the stress–strain relationships. Fig. 3b shows the average stress–strain relationship of the material up to a tensile strain of 0.0015. From the results, the average Young's modulus of the material was determined to be 3 GPa. Poisson's ratio of the material was assumed to be 0.45 in accordance with the manufacture's data sheet. It should be noted, in the experiments glass failed before the failure of the adhesive or the interfaces, therefore the ultimate strength and the failure mechanisms of Araldite 2020 were not required in the FE models.

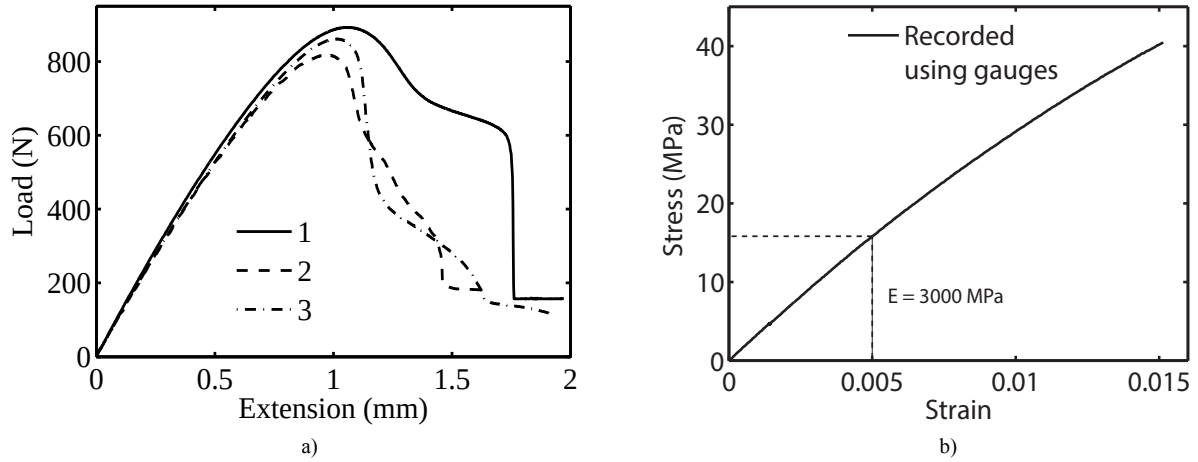

Fig. 3 a) Load-displacement curve of adhesive tensile testing, b) Stress–strain relationship of Araldite 2020.

Material mechanical used in the FE models of the beams are summarised in Table 1.

Table 1: Mechanical properties of the materials.

Material	Young's Modulus [GPa]	Poisson ratio
Glass	70	0.23
GFRP	24.5	0.10
Araldite 2020	3	0.45

5. Results and Discussion

5.1. Single Layer Glass Beams

As expected, single layer glass beams failed in brittle manner due to the formation of a major crack in the constant moment zone. Three single layer beams were tested; all specimens showed a similar linear behaviour until the failure. The failure load of the three beams were determined to be 0.42, 0.48 and 0.41 kN, giving an average failure load of 0.44 kN. The variance in the observed failure load of the three beams are well within the scatter of test results usually reported in the literature (e.g. Veer et al 2008). Fig 4a shows the load–midspan deflection relationship of one beam specimen. The figure also shows the prediction from the FE analysis. The comparison shown in Fig. 4a suggest that the results of the FE model agree with the experimental results where the difference in the predicted and the actual stiffness of the beam is less than 10%.

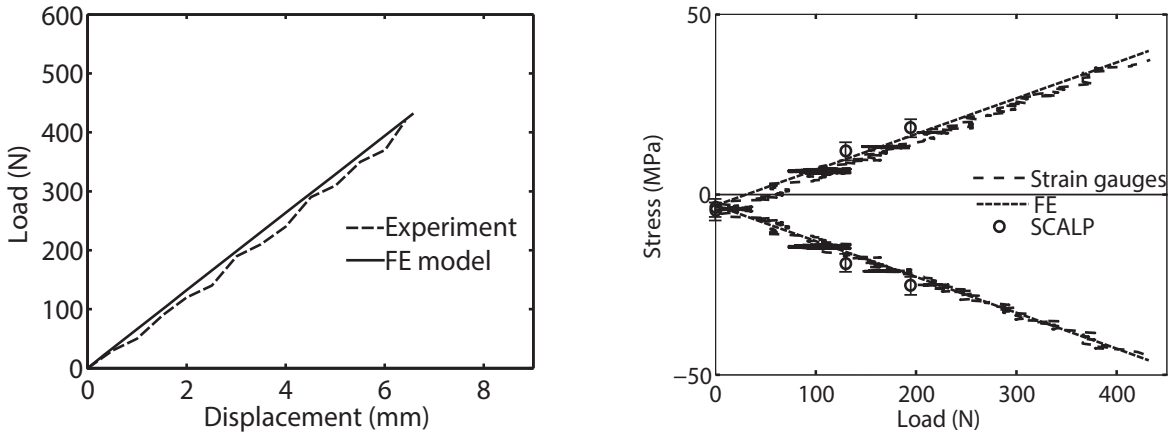

a) b)

Fig. 4 a) Load–midspan deflection curve for single layer glass beam, b) Stress at the tension and compression surfaces.

Fig. 4b presents the longitudinal stresses calculated at the tension (positive) and the compression (negative) surfaces using the readings of the strain gauges and SCALP-05. The figure also shows the predictions from the FE model. The figure presents the data for one beam only; the results of other two beams are similar. It should be noted that the readings obtained from the strain gauges were adjusted to ensure that measured strains match with the initial compressive residual stress of 3.5 MPa at the both top and bottom surfaces (Achintha and Balan 2015). From the figure, it can be seen that once the loading has started, the stresses started to increase linearly until the failure. The stress measurements using SCALP-05 were made at two load values well before the failure of the beams. The results suggest that stresses calculated from the strain gauge data agree well with the stress data obtained from SCALP-05. The results also suggest that the stresses predicted by the FE model match well with the experiments. The discrepancy between the predicted values and the experimental results are less than 10%. The compressive surface stress (calculated using the measured strain data) at the failure of the three beams are 44.5 MPa, 50 MPa and 41 MPa. The corresponding failure stresses at the tension surface are 39 MPa, 40.8 MPa and 37.4 MPa. These experimentally calculated values match well with the predicted failure stresses in the FE analysis: 46 MPa (compression) and 39.9 MPa (tension).

5.2. Double Layer Glass Beams

Fig. 5a shows the load–midspan deflection relationship of one double layer glass beam. It should be noted that all three double layer beams showed similar behaviours to that shown in Fig. 5a. As expected, the double layer beams had higher stiffness (about 7 times that of single layer beams) and higher load capacity (average failure load = 1.52 kN) than the single layer beams (average failure load = 0.44 kN). However, the beams failed in the same brittle manner as the single layer beams due to a major crack originated in the bottom glass sheet in the constant moment zone. The adhesive layer, which bonded the two glass sheets, did not carry the load after the first failure of the beam.

Fig. 5a also shows the load–midspan deflection predicted from the FE analysis for the double layer glass beams. The results suggest that the FE analysis overestimated the flexural stiffness of the beams. The authors believe this discrepancy is attributed to the assumption of the full strain compatibility between glass and adhesive. However, the predictions from the FE analysis for the failure load and final deflection of the beams do not differ by more than usually expected variance of 20% of the average values.

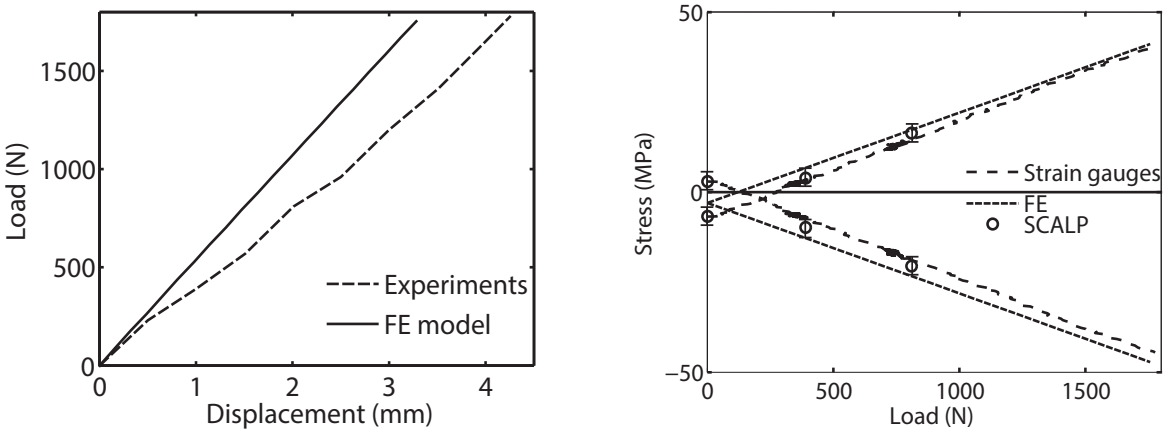

a) b)

Fig. 5 a) Load–midspan deflection curve for adhesively bonded double layer glass beam, b) Stress at the tension and compression surfaces.

Fig 5b shows the stresses determined from the strain gauge readings and SCALP-05 at the tension and compression surfaces of one of the double layer glass beams. It should be noted that owing to the manufacturing process used to fabricate the beams, the initial stress states in the double layer beam was different to that presented in the single layer beams. Using the SCALP-05, it was determined that the initial stress at the bottom surface was 6 MPa (compression) whereas that at the top surface was 3 MPa (tension). Once the loading started the stress increases linearly until the failure of the beam at applied load ~1.6 kN. Using the recorded strain data the surface stresses at the failure were determined to be 40 MPa and 44.5 MPa at the tension and the compression surfaces respectively. The corresponding average values of the three test beams are 37 MPa (tension) and 44 MPa (compression). As can be seen from Fig 5b, the stress values measured using SCALP-05 match with the stress determined from the strain data. Fig. 5b also shows that the predictions from the FE model agree well with the stresses calculated from the experiments. The failure load predicted by the FE model (1.7 kN) matches well with the experimentally observed average failure load of 1.52 kN. The FE predicted stress values of 41.1 MPa at the tensile surface and 47 MPa at the compression surface at the predicted failure load agree well with the respective average measured values of 37 MPa (tension) and 44 MPa (compression).

5.3. Glass–GFRP Hybrid Beams

Three identical glass–GFRP hybrid beams fabricated as described in Section 2.3 were tested. As expected, the beams showed linear behaviour similar to other types of beams until the formation of the first major crack. However, unlike other beams, the hybrid beams did not lose the load carrying capacity or the stiffness completely. Fig. 6a shows the measured load–midspan deflection relationship of one of the hybrid beams; all three test beams showed similar behaviour, with reported maximum loads 2.62 kN, 2.07 kN and 2.04 kN giving an average value of 2.25 kN. As it can be seen from Fig. 6a, after the first major crack, the load dropped by ~50% to ~1 kN and the midspan deflection increased by ~20 %. The beams were tested under displacement controlled, and after the first major crack the beam started to take more load. Despite the continuous decrease in the stiffness due to the development of new cracks, the beam resisted load up to 1.5 kN (~70 % of the previous maximum load). Once the bottom glass layer has cracked, the GFRP layer carried the tension and also held the already broken glass pieces together ensuring a stiffness in the cracked beam. The tests were stopped when the midspan deflection reached 25 mm. As depicted in Fig 6a, an important characteristic of the hybrid beams was that upon unloading the beam almost recovered fully. Fig. 6a also shows that the load–midspan deflection relationship and the maximum load predicted by the FE model (2.20 kN) for the uncracked behaviour of the beam agree well with the experiments.

Fig. 6b shows the stresses determined from the strain gauge data and SCALP-05 at the tension and compression surfaces of one of the hybrid beams before the development of the first major crack. Using SCALP-05, it was determined that the initial stress at the bottom (tension) surface of the beam was 8 MPa (compression) whereas that at the top (compression) surface was 4 MPa (tension). Once the loading started the stress increases linearly until the first cracking of the beam at applied load ~2 .07 kN. Using the recorded strain data the surface stresses at the peak load were determined to be 37 MPa (tension) and 42 MPa (compression). Similar values of stresses were noted in other two test beams. As can be seen from Fig 6b, the stresses measured using SCALP-05 match with that determined from the strain data. Fig. 6b also shows that predictions from the FE model agree well with the

experimentally determined stresses. The maximum load predicted by the FE model (2.20 kN) matches with the experimentally observed average maximum load of 2.07 kN. The FE predicted peak stresses of 41.3 MPa (tension) and 47.2 MPa (compression) at the predicted maximum load also agree well with the respective experimentally determined stresses of 37 MPa (tension) and 42 MPa (compression).

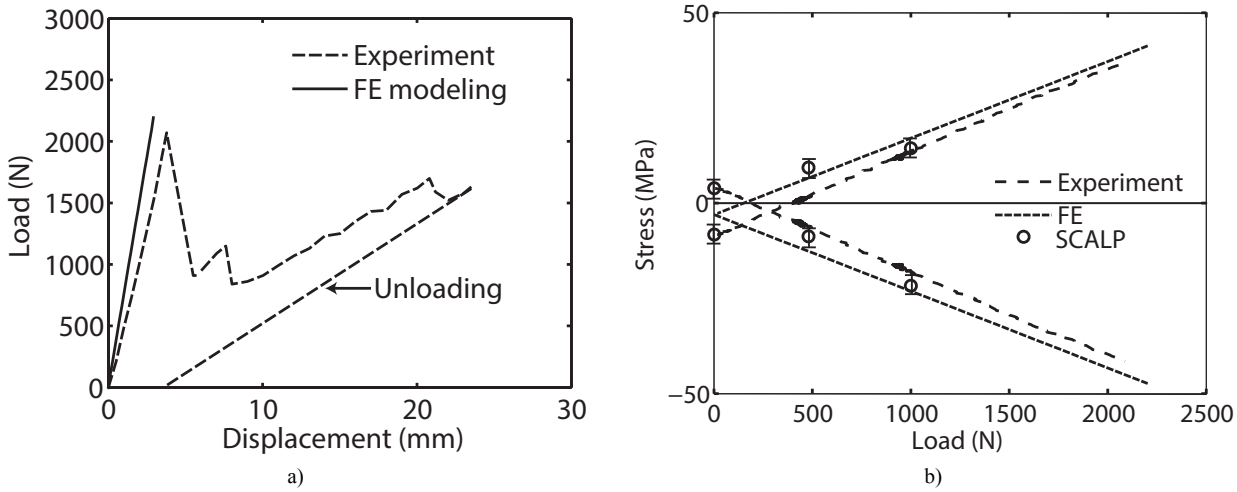

a) b)

Fig. 6 a) Load–midspan deflection curve for glass–GFRP hybrid beam, b) Stress at the tension and compression surfaces.

6. Post-Fracture Behaviour and Ductility of Glass–GFRP Hybrid Beams

Fig.7a summarises the load–midspan deflection relationship of the single layer and double layer glass beams, and the hybrid beams. As depicted in the figure, unlike the single and double layer glass beams where both beams failed in brittle manner at the maximum load, the hybrid beams continued to take load after the first major crack albeit a drop in the stiffness. As described in Section 5.3, once the bottom glass layer has cracked the combination of the GFRP and the top glass layer carried the applied load whilst the stiffness of the beam gradually decreased due to the development of new cracks. Fig. 7b illustrates that despite the heavy cracking the hybrid beams recovered the deflection upon unloading.

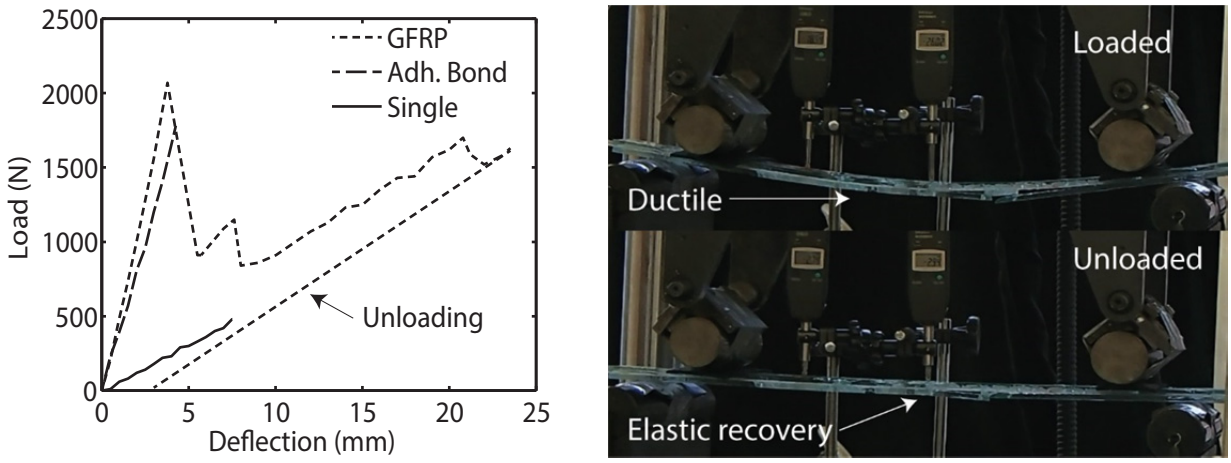

a) b)

Fig. 7 a) Comparison of load–midspan deflection curves of different types of beams, b) Cracked hybrid beam after unloading.

A ductility index, the ratio of the additional midspan deflection after the first major crack in the beam to the midspan deflection at the first major crack in the beam, may be used to quantify the ductility of the hybrid beams. The hybrid beams has a ductility index greater than 7.2, whereas that of single and double layer glass beams is zero since both beams failed in brittle manner at the maximum load.

Table 2 summarises the average maximum load, percentage increase in the maximum load with respect to that of the single layer beams, surface tensile stress at the first major crack, and the ductility index, of all types of beams. From the table it can be seen that double layer glass beams and the hybrid beams and are about 3.5 and 5 times stronger than the single layer beams respectively. However, it should be noted that the tensile stress in the bottom glass layer at the respective peak load of all beams are similar, 37–39 MPa (Table 2). This indicates that, as expected, the adhesive and the GFRP had no influence in improving the strength of glass, but the overall load capacity increased

due to the use of GFRP interlayer. The results confirm that the use of adhesively-bonded GFRP interlayer enables the development of stronger and ductile hybrid beams compared to conventional single and multilayer float glass beams.

Table 2: Load, ductility index and percentage increase for different types of beams.

Beam type	Maximum load [kN]	Surface tensile stress [MPa]	Ductility index (DI)	Percentage increase in peak load [%]
Single layer	0.44	39	0	-
Double layer	1.52	37	0	345
Glass–GFRP hybrid	2.25	37	> 7.2	511

7. Conclusions

The experiments showed that double layer float glass–GFRP hybrid beams continued to take load even after the formation of the first major crack. Once the bottom glass layer has cracked, the combination of the GFRP and the top glass layer carried the applied load whilst the gradual decrease in the stiffness due to the formation of new cracks ensures a ductile failure. The experiments also showed that despite the heavy cracking, the hybrid beams recovered almost the total deflection upon unloading.

The results confirm that the use of adhesively-bonded GFRP interlayers enable the development of float glass–GFRP hybrid beams which are stronger and ductile than conventional single and multilayer float glass beams.

The experiments also showed that Araldite 2020 is a viable structural adhesive that ensures sufficient composite behaviour in glass–GFRP hybrid beams.

Experimentally-validated finite element (FE) models have been presented that predict the evolution of stresses, stiffness and failure load of single and double layer float glass beams and that of hybrid beams.

Acknowledgements

Funding from the University of Southampton and the Institution of Structural Engineers Research Award (2012) are greatly acknowledged.

References

ABAQUS/Standard 6.9-3. Simulia.
Achintha, M., Balan, B.A.: An experimentally validated contour method/eigenstrains hybrid model to incorporate residual stresses in glass structural designs. J. Strain Analysis. 50, 614-627 (2015)
ASTM D3039/D3039M-95. Standard test method for tensile properties of polymer matrix composite materials.
ASTM D638-02. Standard test method for tensile properties of plastics.
Balan, B.A., Achintha, M: Assessment od stresses in float and tempered glass using eigenstrains. Experimental Mech. 55, 1301-1315 (2015)
Belis, J., Van Hulle, A., Out, B., Bos, F., Callewaert, D., Poulis, H.: Broad screening of adhesives for glass-metal bonds. In: Glass performance days 2011
Blyberg, L., Serrano, E.: Timber/Glass adhesively bonded I-beams. In: Glass Perf. Days (2011)
BS-EN 572-2:2012. Glass in building. Basic soda lime silicate glass products. Float glass.
BS-EN 1288-3:2000. Glass in building – Determination of the bending strength of glass – Part 3: test with the specimen supported at two points.
Correia, J.R., Valarinho, L., Branco, A.: post-cracking strength and ductility og glass-GFRP composites beams. Comp. Struct. 93, 2299-2309 (2011)
Haldiman, M., Luible, A., Overend, M.: Structural use of glass. Zurich, CHE (2008)
Louter, C.: Structural glass beams with embedded glass fibre reinforcement. In: Proc. Challenging Glass 2. (2010)
Louter, C., Belis, J., Veer, F., Lebet, J.P.: Structural response of SG-laminated reinforced glass beams; experimental investigations on the effect of glass type, reinforcement percentage and beam size. Eng. Struct. 36, 292-301 (2012)
Nielsen, J.H., Olesen, J.F.: Post-crack capacity of mechanically reinforced glass beams. In: Proc. of Fra. Mech. Concrete. Struct 370-376 (2010)
OLYMPUS instruction manual. Olympus Europa Holding GMBH.
SCALP instruction manual, ver. 5.0. GlasStress Ltd.
Speranzi, E., Agnetti, S.: Flexural performance of hybrid beams made of glass and pultruded GFRP. Const. Building Mat. 94, 249-262 (2015)
The Institution of Structural Engineers: Structural use of glass in buildings. London, UK (2014)
Veer, F.A., Louter, P.C., Bos, F.P.: The strength of annealed, heat-strengthened and fully tempered float glass. Fatigue Fract. Eng. Mat. Struct. 32, 18-25 (2008)